A severe defect in CRAC Ca^{2+} channel activation and altered K^+ channel gating in T cells from immunodeficient patients

Stefan Feske,[1] Murali Prakriya,[2] Anjana Rao,[1] and Richard S. Lewis[2]

[1]CBR Institute for Biomedical Research and Department of Pathology, Harvard Medical School, Boston, MA 02115
[2]Department of Molecular and Cellular Physiology, Stanford University School of Medicine, Stanford, CA 94305

Engagement of the TCR triggers sustained Ca^{2+} entry through Ca^{2+} release-activated Ca^{2+} (CRAC) channels, which helps drive gene expression underlying the T cell response to pathogens. The identity and activation mechanism of CRAC channels at a molecular level are unknown. We have analyzed ion channel expression and function in T cells from SCID patients which display 1–2% of the normal level of Ca^{2+} influx and severely impaired T cell activation. The lack of Ca^{2+} influx is not due to deficient regulation of Ca^{2+} stores or expression of several genes implicated in controlling Ca^{2+} entry in lymphocytes (*kcna3*/Kv1.3, *kcnn4*/IKCa1, *trpc1*, *trpc3*, *trpv6*, *stim1*). Instead, electrophysiologic measurements show that the influx defect is due to a nearly complete absence of functional CRAC channels. The lack of CRAC channel activity is correlated with diminished voltage sensitivity and slowed activation kinetics of the voltage-dependent Kv1.3 channel. These results demonstrate that CRAC channels provide the major, if not sole, pathway for Ca^{2+} entry activated by the TCR in human T cells. They also offer evidence for a functional link between CRAC and Kv1.3 channels, and establish a model system for molecular genetic studies of the CRAC channel.

CORRESPONDENCE
Richard S. Lewis:
rslewis@stanford.edu

Abbreviations used: 2-APB, 2-aminoethyldiphenyl borate; Ca_V, voltage-gated Ca^{2+}; CRAC, Ca^{2+} release-activated Ca^{2+}; CTX, charybdotoxin; DVF, divalent-free; I_{CRAC}, CRAC current; MIC, Mg^{2+}-inhibited cation; PLC, phospholipase C; PMCA, plasma-membrane Ca^{2+}-ATPase; ShK toxin, *Stichodactyla helianthus* toxin; STIM, stromal interaction molecule; TG, thapsigargin; TRP, transient receptor potential.

Ca^{2+} has an essential role during development and for the mature function of lymphocytes. In mature T lymphocytes, presentation of antigen triggers a coordinated series of events culminating in cell activation and proliferation. One of the earliest biochemical steps in this process is the activation of phospholipase C (PLC)γ, which generates inositol-1,4,5 trisphosphate, releasing Ca^{2+} from the ER. The resulting decrease in lumenal ER Ca^{2+} triggers Ca^{2+} influx by opening a class of store-operated Ca^{2+} channels in the plasma membrane, known as Ca^{2+} release-activated Ca^{2+} (CRAC) channels (1–3). The ensuing sustained $[Ca^{2+}]_i$ elevation activates transcriptional pathways required for proliferation and effector immune function. Ca^{2+} also has an essential role in T cell development, by influencing thymocyte motility and positive selection (4, 5). Pharmacologic, electrophysiologic, and genetic evidence support the notion that CRAC channels are the principal pathway for Ca^{2+} influx in developing and mature T cells, and thus, are likely to orchestrate many aspects of lymphocyte development and function (3). The importance of store-operated Ca^{2+} entry for immunologic host defense is highlighted by the severe deficiencies in T cell activation and effector gene expression in patients lacking store-operated Ca^{2+} entry (6–8). Thus, understanding the functional and molecular properties of CRAC channels is central to a complete understanding of T cell activation.

Several of the key downstream signaling pathways triggered by CRAC channel activity have been defined, but the molecular identity of the CRAC channel and its activation mechanism remain elusive. Several candidate genes belonging to the transient receptor potential (TRP) family of ion channels have been proposed to encode the CRAC channel, including *trpc1* (9), *trpc3* (10), and *trpv6* (11, 12), as well as voltage-gated Ca^{2+} (Ca_V) channels (13, 14). However, evidence that TRPs are store-dependent following heterologous expression in several cell lines is inconsistent (15, 16), and none of the candidates exhibits all of the key biophysical hallmarks of the CRAC channel: lack of significant voltage-dependent gating, an extremely high selectivity for Ca^{2+} over monovalent cations, extremely low single-channel

S. Feske and M. Prakriya contributed equally this work.
The online version of this article contains supplemental material.

Supplemental material can be found at:
http://doi.org/10.1084/jem.20050687

conductance (<1 pS), inwardly rectifying current-voltage relationship, rapid Ca^{2+}-dependent inactivation, blockade by submicromolar La^{3+}, and modulation by 2-aminoethyldiphenyl borate (2-APB; references 3, 17, 18). Thus, homomultimers of these TRPs or Ca_V proteins are unlikely to make up the native CRAC channel. Likewise, the nature of the signal that links store depletion to channel activation is unknown, despite a large number of proposed mechanisms (16).

Cells with a specific defect in the CRAC channel or its activation process would provide a much-needed system for elucidating the molecular basis of CRAC channel function. We previously described two SCID patients with impaired T cell activation arising from reduced activity of NFAT (19), which was shown to result from a marked deficit in store-operated Ca^{2+} entry (8). In principle, this deficit could reflect abnormalities in any of several processes related to Ca^{2+} influx, including ER Ca^{2+} store regulation and the activity of K^+ channels in addition to CRAC channels themselves. K^+ channels have long been known to play a critical role in early events in T cell activation, most likely by maintaining a negative resting potential that provides the electrical driving force for Ca^{2+} entry (20). Pharmacologic blockade of K^+ channels profoundly inhibits T cell activation, an effect that has been ascribed to membrane depolarization and a consequent reduction of the driving force for Ca^{2+} entry through CRAC channels (21). Here we show that the lack of Ca^{2+} signaling results directly from a selective absence of CRAC channel activity, most likely due to aberrant CRAC channel regulation. Expression of other channels, including TRPC1, TRPC3, TRPV6, TRPM7, and the K^+ channels, IKCa1 and Kv1.3, is normal. However, the gating properties of the voltage-gated K^+ channel Kv1.3 are altered in the SCID T cells. Collectively, these results establish the SCID T cells as a model system for identifying molecules involved in CRAC channel activation, and reveal a possible functional link between CRAC channels and K^+ channel gating.

RESULTS

Store-operated Ca^{2+} entry is deficient in SCID cells despite normal Ca^{2+} release from stores

We previously described a Ca^{2+} signaling defect in T lymphocytes from patients with a SCID (8, 19, 22). This defect nearly abolished Ca^{2+} influx in the SCID T cells following activation of TCR and after passive depletion of intracellular Ca^{2+} stores with thapsigargin (TG) or ionomycin. Because Ca^{2+} store depletion is necessary for any of these stimuli to activate Ca^{2+} influx through CRAC channels, we asked whether Ca^{2+} stores are abnormal in the SCID T cells—either in their content or their ability to release Ca^{2+}. Treatment of SCID T cells with anti-CD3 mAb (Fig. 1 A) or TG (Fig. 1 B) in the absence of extracellular Ca^{2+} evoked the normal extent of Ca^{2+} release from intracellular stores compared with control T cells from healthy individuals, as measured by the amplitude and kinetics of the $[Ca^{2+}]_i$ increase. In both cases, readdition of 2 mM $Ca^{2+}{}_o$ to the SCID T cells failed to elicit significant Ca^{2+} influx compared with control

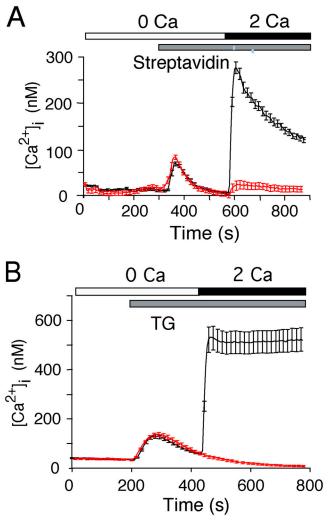

Figure 1. Ca^{2+} store depletion fails to activate significant Ca^{2+} entry in T cells from SCID patients. (A) Intracellular Ca^{2+} release and influx in response to CD3 cross-linking in T cells from healthy controls (black trace; $n = 30$ cells) and SCID patients (red trace; $n = 30$ cells). Biotinylated anti-CD3 antibody (5 μg/ml) was cross-linked with streptavidin (5 μg/ml) as indicated in the absence of extracellular Ca^{2+} to measure intracellular Ca^{2+} release, followed by addition of 2 mM Ca^{2+} to measure influx. (B) Ca^{2+} release and influx stimulated by TG (1 μM) in T cells from healthy controls (black trace; $n = 30$ cells) and SCID patients (red trace; $n = 30$ cells). In both experiments, Ca^{2+} influx in SCID cells largely is absent despite normal release of Ca^{2+} from stores.

cells, as documented previously (8). Thus, the defect in Ca^{2+} influx is not the result of aberrant Ca^{2+} store depletion in the SCID T cells.

Consistent with these results, the expression of PLCγ1 and γ2 and inositol-1,4,5 trisphosphate receptors—proteins that link TCR stimulation to store depletion—in SCID T cells was within the range of protein expression in control T cells (Fig. S1, available at http://www.jem.org/cgi/content/full/jem.20050687/DC1). Together, these results demonstrate normal operation of the Ca^{2+} signaling machinery leading from TCR engagement to Ca^{2+} release from the ER, and suggest that the absence of store-operated Ca^{2+} influx in the SCID T cells is due to a defect downstream of Ca^{2+} store depletion.

Store depletion fails to activate CRAC channels in SCID T cells

In principle, several mechanisms could abrogate Ca^{2+} influx subsequent to store depletion. These include defective expression or function of store-operated CRAC channels, as well as less direct mechanisms involving depolarization of the cell's membrane potential and consequent reduction of the driving force for Ca^{2+} entry. To distinguish between these possibilities, we directly measured CRAC channel function in SCID patients and control T cells using the whole-cell patch-clamp technique.

Control and SCID T cells were pretreated with 1 μM TG for 15 min to deplete Ca^{2+} stores completely. Subse-

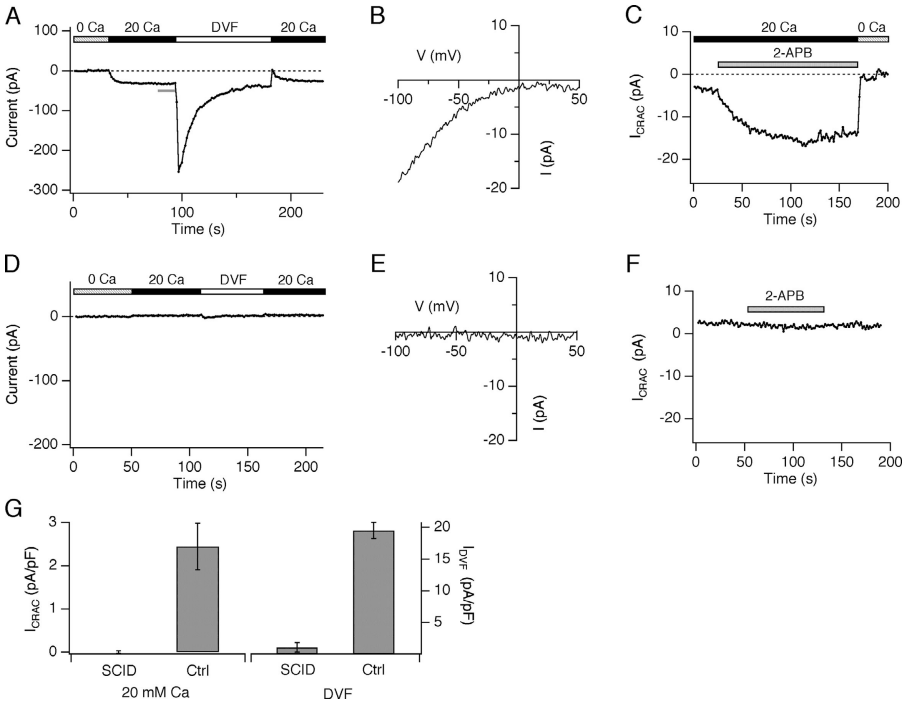

Figure 2. Functional CRAC channels are undetectable in whole-cell patch-clamp recordings from SCID T cells. (A) Ca^{2+} and Na^+ currents through CRAC channels in a control T cell. Peak currents recorded every 1.5 s during brief steps to −110 mV are shown. Exposure of this TG-pretreated cell to 20 mM Ca^{2+} evoked an inward CRAC Ca^{2+} current, whereas subsequent exposure to DVF solution allowed Na^+ to carry an approximately eightfold larger inward current that declined slowly due to depotentiation. (B) Current-voltage relationship of the CRAC Ca^{2+} current. The graph shows the average of 10 leak-corrected responses to voltage ramps recorded from 78–92 s shown by the gray bar in A. (C) 2-APB strongly enhanced I_{CRAC}. After development of I_{CRAC}, 5 μM 2-APB was applied as indicated. Peak currents at −110 mV plotted as in A. (D) CRAC Ca^{2+} and Na^+ currents were absent in SCID T cells. Same protocol as in A. (E) Current-voltage relationship of the current recorded in D. (F) Application of 5 μM 2-APB failed to elicit a response in the SCID cells. (G) Summary of the Ca^{2+} (I_{CRAC}) and Na^+ (I_{DVF}) current densities in control (Ca^{2+} current: $n = 5$ cells; Na^+ current: $n = 4$ cells) and SCID (Ca^{2+} current: $n = 6$ cells; Na^+ current: $n = 4$ cells) T cells normalized to the capacitance of each cell (a measure of surface area).

quent exposure of control T cells to 20 mM Ca^{2+} produced an inward Ca^{2+} current in 5/5 cells (Fig. 2 A), which was identified as CRAC current (I_{CRAC}) based on several key characteristics. First, the response to rapid voltage ramps showed an inwardly rectifying current-voltage relationship and lack of an obvious reversal potential, both of which are typical of I_{CRAC} (Fig. 2 B). Second, as previously shown for I_{CRAC} in Jurkat T cells (23), the Ca^{2+} current in normal human T cells was potentiated strongly by 5 μM 2-APB (240 ± 45% enhancement; $n = 4$ cells; Fig. 2 C). Third, removal of all extracellular Ca^{2+} and Mg^{2+} by application of a divalent-free (DVF) solution produced an inward Na^+ current that initially was approximately eightfold larger than the preceding Ca^{2+} current, and slowly declined by ~90% (Fig. 2 A). It is well known that removal of divalent cations allows Na^+ to permeate CRAC channels but does not sustain their activity, leading to a slow rundown of the current in Jurkat T cells (24, 25) and RBL cells (26).

In contrast to the control cells, TG-pretreated SCID T cells exhibited no detectable I_{CRAC} in 20 mM $Ca^{2+}{}_o$ (Fig. 2, D and E; 6/6 cells). Currents were not increased, even after removal of extracellular divalent cations (Fig. 2, D and G) or after treatment with 5 μM 2-APB (Fig. 2 F), two conditions that greatly enhance the sensitivity for detecting current through normal CRAC channels. These results directly demonstrate an extreme lack of functional CRAC channels in the SCID T cells that can account for the profound defects in Ca^{2+} influx observed after stimulation through the TCR or after passive store depletion.

Residual Ca^{2+} influx in SCID T cells: evidence for a defect in CRAC channel activation

The absence of CRAC channel activity in SCID T cells could arise from two potential sources: aberrant expression of CRAC channels (e.g., a null mutation in the structural gene for the channel or faulty trafficking to the plasma membrane) or defective activation of CRAC channels in response to store depletion. Clues that distinguish between these mechanisms came from observations of residual Ca^{2+} influx in the presence of high extracellular Ca^{2+} levels. Although store-depleted SCID cells fail to display detectable I_{CRAC} and lack Ca^{2+} influx in 2 mM $Ca^{2+}{}_o$, they do exhibit a small degree of Ca^{2+} influx in the presence of 20 mM $Ca^{2+}{}_o$. This influx occurred in all SCID cells, and evoked a transient increase in $[Ca^{2+}]_i$ (Fig. 3 A). The initial slope of the $[Ca^{2+}]_i$ increase was measured as an indicator of the apparent Ca^{2+}

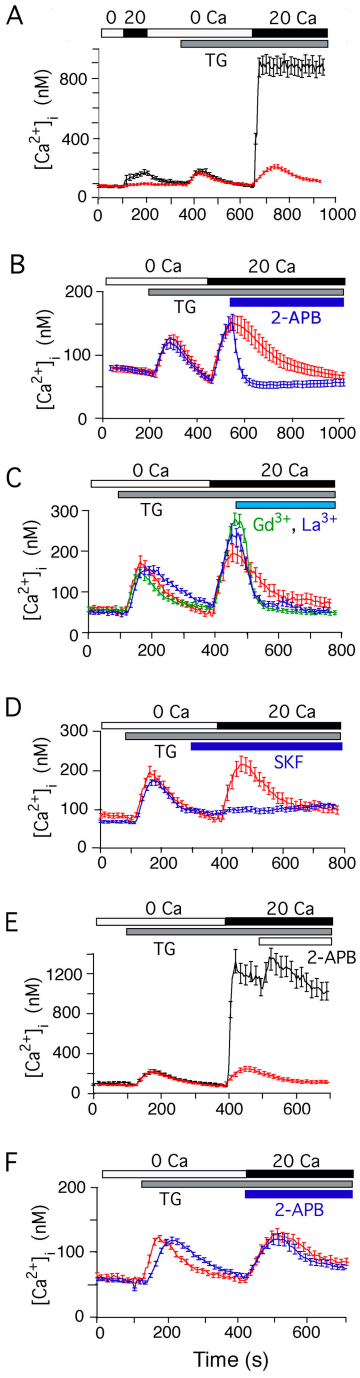

Figure 3. Residual Ca^{2+} influx in SCID T cells is due to CRAC channels with an altered sensitivity to 2-APB. (A) Residual Ca^{2+} influx in SCID cells is store-dependent. Exposure to 20 mM Ca^{2+} before treatment with TG elicits a small $[Ca^{2+}]_i$ increase in control (black trace) but not SCID T cells (red trace). The small influx in control cells may reflect a low level of CRAC channel activity induced by previous incubation in 0 Ca^{2+}. Following store depletion with TG, readdition of 20 mM Ca^{2+} caused a small transient $[Ca^{2+}]_i$ increase in SCID T cells; the initial rising phase indicates an influx rate ~1.5% of that in control T cells (also see Fig. S2 A). (B) Residual Ca^{2+} influx is sensitive to inhibition by a high concentration of 2-APB. Addition of 2-APB (75 μM; blue trace) blocked Ca^{2+} entry and caused $[Ca^{2+}]_i$ to decline rapidly in contrast to untreated SCID T cells (red trace). (C) Residual Ca^{2+} influx was inhibited by Gd^{3+} (green trace) or La^{3+} (blue trace; 2 μM). (D) Inhibition of residual Ca^{2+} influx by SKF 96365. Application of SKF 96365 (30 μM) before readdition of Ca^{2+} completely prevented the increase in $[Ca^{2+}]_i$ (blue trace). (E, F) A low concentration of 2-APB failed to enhance residual Ca^{2+} influx in SCID T cells. (E) 3 μM 2-APB enhanced Ca^{2+} influx in control T cell (black trace), but did not affect the Ca^{2+} transient in SCID cells (red trace). (F) 2-APB (5 μM; blue trace) added with 20 mM Ca^{2+} did not increase the Ca^{2+} influx rate, as indicated by the initial slope ($d[Ca^{2+}]_i/dt$), or the peak Ca^{2+} response beyond that seen in untreated SCID T cells (red trace). Plots in A–F show the average and SEM values from 30 cells.

influx rate, which in SCID cells was 1–2% of the rate observed in control T cells under similar conditions (Fig. S2 A, available at http://www.jem.org/cgi/content/full/jem.20050687/DC1). The transient time course of the response is similar to that observed in TG-treated normal Jurkat T cells after initiating influx with low concentration of Ca^{2+}_o (27); most likely this is due to a slow increase in Ca^{2+} extrusion by the plasma membrane Ca^{2+}-ATPase (PMCA), because delayed modulation of PMCA has been shown to create a transient $[Ca^{2+}]_i$ increase in response to constant Ca^{2+} influx through CRAC channels (28).

To examine whether the residual influx represents CRAC channels or a different Ca^{2+} influx pathway, we tested its dependence on store depletion and its sensitivity to CRAC channel inhibitors. Before store depletion by TG, application of 20 mM Ca^{2+}_o did not alter $[Ca^{2+}]_i$ in SCID T cells (Fig. 3 A), indicating that the residual influx in TG-treated cells depends on store depletion. A dose of 2-APB, which fully inhibits I_{CRAC} (75 μM) (23), caused a rapid return of $[Ca^{2+}]_i$ to baseline when applied at the peak of the Ca^{2+} transient, indicating a complete inhibition of residual Ca^{2+} influx (Fig. 3 B). When 2-APB (75 μM) was added at the time of readdition of Ca^{2+}, it completely blocked the residual Ca^{2+} influx in the SCID T cells (Fig. S2 B). Likewise, 2 μM La^{3+} or 2 μM Gd^{3+} rapidly terminated residual Ca^{2+} influx (Fig. 3 C). Although La^{3+} and Gd^{3+} block several types of ion channels, including many TRP channels, at low μM concentrations these trivalent ions are relatively selective inhibitors of CRAC channels (29, 30). Finally, SKF 96365 (30 μM), another inhibitor of CRAC channels (31), accelerated the return of $[Ca^{2+}]_i$ to baseline when added near the peak of the transient (unpublished data). This effect was not as pronounced as the effect of 2-APB or trivalent cations, perhaps because inhibition of CRAC channels by SKF 96365 takes tens of seconds (31). For this reason, we also added the drug ~100 s before readdition of Ca^{2+}, which completely prevented the subsequent Ca^{2+} influx response (Fig. 3 D). Thus, the residual Ca^{2+} influx is store-dependent and displays several pharmacologic hallmarks of the CRAC channel, suggesting that it arises from a small number of open CRAC channels.

A distinctive property of CRAC channels is that their activity is enhanced by low concentrations (1–5 μM) of 2-APB (23). Accordingly, 2-APB (3 μM) added to control T cells following Ca^{2+} readdition caused a distinct further increase in

$[Ca^{2+}]_i$ (Fig. 3 E). Given that the residual Ca^{2+} influx in SCID T cells displays several key properties of the CRAC channel, it was surprising that 2-APB at low concentrations (≤5 μM) failed to enhance residual influx when added near the peak of the Ca^{2+} transient (Fig. 3 E). A similar lack of effect was noted when 2-APB was added at a longer time (240 s) following Ca^{2+} readdition (unpublished data). To maximize the detectability of a change in influx rate, we also added 2-APB simultaneously with Ca^{2+}; under these conditions, 2-APB also failed to enhance the rate of Ca^{2+} influx in SCID T cells (Fig. 3 F; 0.90 nM/s versus 0.87 nM/s with or without 5 μM 2-APB, respectively). The inability of low concentrations of 2-APB to enhance residual Ca^{2+} influx in SCID cells cannot be explained by a defect that simply reduces the number of CRAC channels in the plasma membrane, because a small number of normal channels in the membrane would be expected to show normal enhancement by 2-APB (e.g., see Fig. 2 C). Enhancement of I_{CRAC} by 2-APB is believed to involve augmentation of the activation process (32). Thus, an alternative explanation of our findings is that the SCID cells have a primary defect in the CRAC channel activation process, such that overall activity and enhancement are only 1–2% of the control level. Such a defect in SCID cells could arise from abnormal generation or response to the activation signal (see Discussion).

A primary defect in the activation, rather than the expression or targeting, of CRAC channels also is consistent with a molecular analysis of potential CRAC channel genes in the SCID cells. A variety of genes in the *trp* family, including *trpc1* (9), *trpc3* (10), *trpc4* (33), and *trpv6* (11, 12) have been proposed to form parts of store-operated Ca^{2+} channels, in general, or the CRAC channel, in particular. We found that transcripts for *trpc1*, *c3*, *c4*, *c5*, *c7*, *trpv5*, and *v6*, are present in control T cells and at similar levels in SCID T cells (Fig. S3, available at http://www.jem.org/cgi/content/full/jem.20050687/DC1). In addition, no mutations were detected in transcripts of *trpc1*, *c3*, *m2*, *v5*, or *v6* amplified by RT-PCR or in gene loci, including all known exons and splice junctions for *trpc3*, *c5*, *c6*, *m5*, *v5*, *and v6* using DNA from both patients, their parents, one healthy brother, and one independent control (unpublished data). Furthermore, patients were heterozygous by haplotype mapping for the

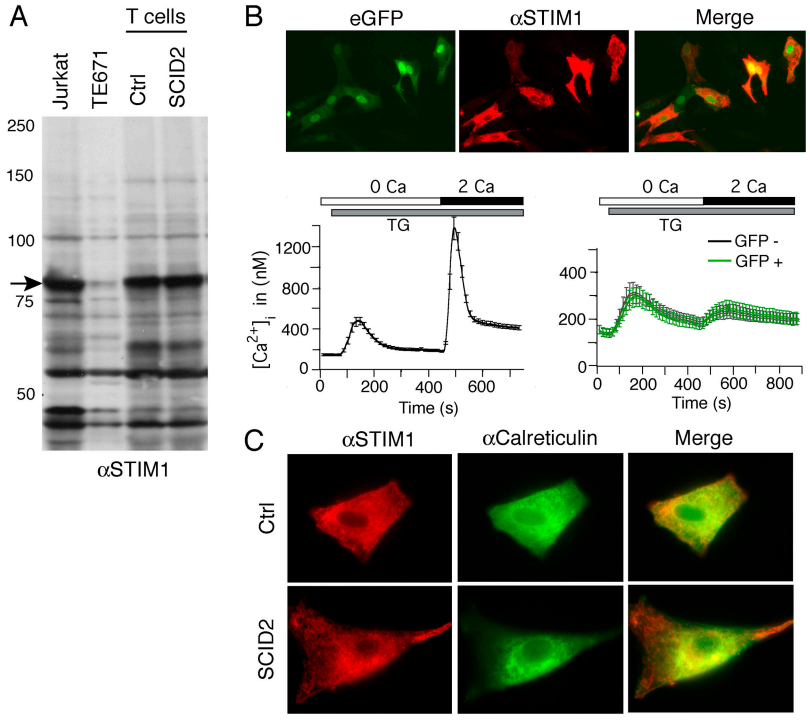

Figure 4. The lack of store-operated Ca^{2+} influx in SCID cells is independent of STIM1 expression. (A) STIM1 protein expression in SCID T cells. Whole-cell lysates from control and SCID patients' T cells, Jurkat, and TE671 cells were immunoblotted with αSTIM1 mAb, detecting a dominant band at 80–85 kD. (B) Exogenous expression of STIM1 fails to rescue Ca^{2+} influx in SCID fibroblasts. STIM1 was coexpressed with eGFP in fibroblasts from SCID patients (top panels). Virtually all cells expressing eGFP (green) showed a strong STIM1 signal (red) by immunocytochemistry. 48 h after transfection, cotransfected SCID fibroblasts were stimulated with TG (1 μM) in the absence of Ca^{2+} followed by readdition of 2 mM Ca^{2+} (bottom right). Mean Ca^{2+} responses for GFP^+ (green) and GFP^- (black) cells from the same experiment are shown. The Ca^{2+} response in untransfected control fibroblasts (bottom left) is shown for comparison. Results shown are representative of five experiments. (C) STIM1 shows a similar distribution in fibroblasts from SCID patients and controls. STIM1 was expressed in fibroblasts from one control and one SCID patient and protein localization detected by immunocytochemistry 48 h later. Merged images show substantial overlap of STIM1 and calreticulin indicating predominant localization of STIM1 in the ER in control and SCID fibroblasts. Images shown were obtained by deconvolution of an image z-stack.

region containing *trpv5* and *v6* genes on chromosome 7q31, incompatible with the autosomal recessive mode of inheritance in this disease (unpublished data). Finally, retrovirus-based overexpression of myc-tagged TRPV6 failed to restore TG- or TCR-triggered Ca^{2+} influx in SCID T cells or TG-triggered influx in fibroblasts (unpublished data). Collectively, these observations lend further support to the notion that the locus of the SCID defect involves the activation, rather than the expression, of store-operated Ca^{2+} channels.

Given the evidence for a regulatory defect in CRAC channel activation, we examined the expression of stromal interaction molecule (STIM)1, a conserved ER protein recently shown to be essential for CRAC channel activation in multiple cell types (34). Endogenous STIM1 protein levels in T cells from SCID patients were comparable to those of control T cells and Jurkat cells (Fig. 4 A). In addition, no mutations in STIM1 were apparent from sequencing genomic DNA from the SCID patients. To test whether STIM1 overexpression could rescue the Ca^{2+} influx defect in cells from the SCID patients, their fibroblasts were cotransfected with pSTIM1 and GFP. Virtually all GFP^+ cells also expressed STIM1 as determined by immunocytochemistry (Fig. 4 B). However, GFP^+ cells did not show increased store-dependent Ca^{2+} influx compared with GFP^- cells, which—like untransfected SCID fibroblasts and T cells—are Ca^{2+} influx deficient (8). Despite the failure to rescue normal function, STIM1 localization seemed to be similar in transfected SCID and control fibroblasts (Fig. 4 C). Together, these results suggest that the Ca^{2+} influx defect is not due to inadequate expression of STIM1.

Specificity of the CRAC channel defect in SCID T cells

To address the specificity of the CRAC channel defect, we applied patch-clamp techniques to measure the expression and properties of other ion channels in SCID T cells, concentrating on channels known or believed to participate in lymphocyte Ca^{2+} signaling, such as TRPM7 and voltage-gated and Ca^{2+}-activated K^+ channels.

TRPM7 is a widely expressed Ca^{2+}- and Mg^{2+}-permeable ion channel (35, 36). Native TRPM7 channels in T cells, called Mg^{2+}-inhibited cation (MIC) channels or Mg^{2+} nucleotide-regulated metal channels typically are activated by the washout of intracellular Mg^{2+} and ATP during whole-cell recording (25, 35). Because of their slow induction kinetics, MIC channels initially were confused with CRAC channels; however, a variety of evidence argues that they are molecularly distinct (25, 26, 37). In SCID and control T cells, introduction of intracellular Mg^{2+}-free solutions evoked the slow activation of currents with the properties of MIC. As expected for I_{MIC}, the currents showed outward rectification in the presence of extracellular Ca^{2+} and a linear current-voltage relationship reversing around 0 mV in the absence of external divalent ions (Fig. 5 A). The amplitude and activation kinetics of MIC current in SCID T cells also were similar to that of control T cells, demonstrating normal MIC channel expression and properties (Fig. 5 B). The

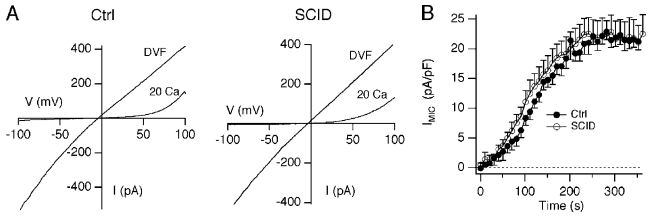

Figure 5. MIC/TRPM7 channels are normal in SCID T cells. (A) Current-voltage relationships showing the typical permeation properties of MIC channels in control (left) and SCID T cells (right). Each graph show currents from one cell after 400 s of whole-cell recording in the presence of 20 mM Ca^{2+} and shortly after removal of divalent ions (DVF solution). (B) Activation kinetics and magnitude of I_{MIC} in SCID T cells are normal. The plot shows peak currents at +100 mV in the presence of 2 mM $Ca^{2+}{}_o$ in control (closed circles; $n = 4$ cells) and SCID T cells (open circles; $n = 5$ cells) as a function of time after break-in with Mg^{2+}-free pipette solution.

nearly complete absence of I_{CRAC} in these cells provides strong genetic evidence that MIC and CRAC currents arise from different gene products.

Human T cells express two classes of K^+ channels: the voltage-gated Kv1.3 channel (encoded by the gene *kcna3*) (38) and the Ca^{2+}-activated IKCa1 channel (encoded by the gene *kcnn4*) (39). Pharmacologic blockade of either type of K^+ channel is known to inhibit Ca^{2+} signaling and T cell function, most likely by causing membrane depolarization and a corresponding reduction in the driving force for Ca^{2+} entry (21). Therefore, it was conceivable that aberrant K^+ channel function contributed to the defect in Ca^{2+} influx in the SCID T cells.

IKCa1 currents were evoked in SCID and control T cells by intracellular dialysis with a buffered solution of 2 μM Ca^{2+} in the presence of equal concentrations of intracellular and extracellular K^+. IKCa1 current was identified in response to voltage ramps from −100 to +100 mV by the increased inward current at membrane potentials negative to −50 mV; at more positive potentials, time- and voltage-dependent activation of Kv1.3 sums with IKCa1 to produce an "N"-shaped current-voltage relation (Fig. 6 A). The current below −50 mV was blocked by 50 nM charybdotoxin (CTX), as expected for IKCa1 channels (39, 40). With 2 μM Ca^{2+} in the pipette solution, the current densities at −100 mV were similar in the control and SCID T cells (Fig. 6 A, right panel), indicating normal IKCa1 expression and function in SCID cells.

Kv1.3 currents were studied in detail using step depolarizations to elicit channel activation. Kv1.3 channels were identified based on a collection of properties, including voltage-dependent activation; cumulative inactivation during a series of repetitive depolarizations; and block by tetraethylammonium, CTX, and the highly selective inhibitor, *Stichodactyla helianthus* (ShK) toxin (41). In all respects, the K_v current in SCID cells was similar to Kv1.3 current in control T cells. Both currents activated at potentials positive to –50 mV with a similar current density (Fig. 6 B) and showed a similar rate

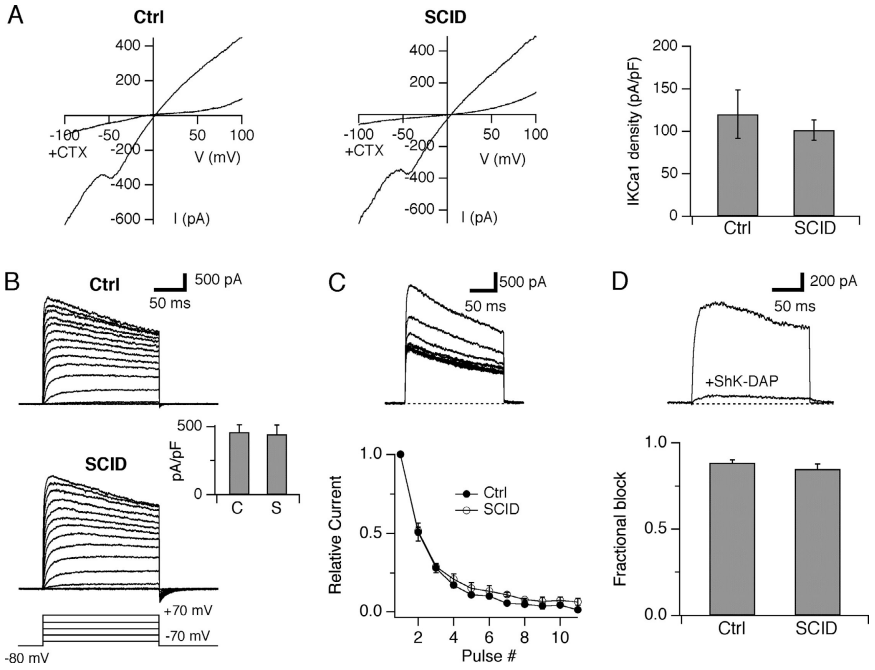

Figure 6. Expression of Ca^{2+}-activated and voltage-gated K^+ channels in SCID T cells. (A) Amplitude of IKCa1 is normal in SCID cells internally dialyzed with 2 μM Ca^{2+}. IKCa1 current density measured from CTX-inhibited currents at −100 mV is plotted for control ($n = 5$ cells) and SCID ($n = 7$ cells) T cells (right). (B) Voltage-dependent K^+ currents in control (top) and SCID T cells (bottom), elicited by depolarizations from −70 to +70 mV in steps of 10 mV. The inset compares peak K^+ current densities at +70 mV in control ($n = 5$ cells) and SCID ($n = 8$ cells) T cells. (C) Cumulative inactivation of Kv1.3 current, elicited by steps to +60 mV applied every 1 s. Top: the first 10 responses to this protocol in a SCID cell. Bottom: average peak currents during successive pulses in control (closed circles; $n = 4$ cells) and SCID cells (open circles: $n = 5$ cells), relative to the first pulse. (D) Inhibition by ShK-Dap[22]. K^+ current in response to a pulse to +60 mV was blocked by 200 pM ShK-Dap[22] in a SCID T cell (top). The degree of block is compared for control ($n = 4$) and SCID ($n = 5$) cells (bottom).

and extent of cumulative inactivation during repetitive pulses to +60 mV (Fig. 6 C). ShK-Dap[22] toxin (200 pM) blocked Kv currents in control and SCID T cells by 88 ± 3% ($n = 5$) and 85 ± 5% ($n = 6$), respectively, consistent with a published K_i of 23 pM (41). In addition, both currents showed similar sensitivity to block by tetraethylammonium and CTX (unpublished data). These results suggest normal functional expression of Kv1.3 channels in the SCID T cells.

Consistent with these results, Kv1.3 transcript levels did not differ significantly between patient and control T cells (Fig. S4 A, available at http://www.jem.org/cgi/content/full/jem.20050687/DC1). Kv1.3 protein was detected readily in patient and control T cells by immunoblotting (Fig. 4S B) and at the cell surface by immunocytochemistry using Kv1.3-specific antibodies (Fig. 4S C, top panels). Flow cytometric measurements of surface binding of fluorescently labeled ShK-F6CA (42) confirmed equivalent surface expression of Kv1.3 in SCID and control T cells (Fig. 4S C, lower panel). β subunits associated with Kv1.3, including Kvβ1, Kvβ2, and Kvβ3, also were expressed normally at the mRNA and protein level (Fig. 4S, A and B).

Kv1.3 channel activation is altered in SCID T cells

Although the expression, inactivation, and pharmacologic profile of Kv1.3 channels was normal in the SCID patient cells, further examination revealed abnormal voltage dependence and kinetics of channel activation. Kv1.3 current in SCID cells showed a normal threshold for activation (approximately −50 mV), but the voltage dependence of channel activation was reduced markedly, as indicated by the diminished slope of the conductance-voltage relation (Fig. 7 A). The K^+ conductance increases *e*-fold per 11 mV in the SCID cells relative to *e*-fold per 6 mV in controls, effectively shifting the voltage for half-maximal activation by ∼12 mV. Altered voltage sensitivity of Kv1.3 channels in the patient cells was accompanied by slower than normal activation and deactivation kinetics (Fig. 7, B and C). These changes in gating seem to be restricted to activation and deactivation; the rate of C-type inactivation of Kv1.3 currents in SCID T cells was normal (Fig. 7 D), consistent with their normal cumulative inactivation characteristics (Fig. 6 C).

DISCUSSION

Here we have identified the underlying basis of the extensive signaling defects in T cells from patients with a rare form of SCID. Previous results revealed a profound lack of TCR-mediated Ca^{2+} influx in these cells, resulting in compromised activation of the phosphatase calcineurin; diminished nuclear translocation of the transcription factor NFAT; and ultimately, the aberrant expression of >100 activation-asso-

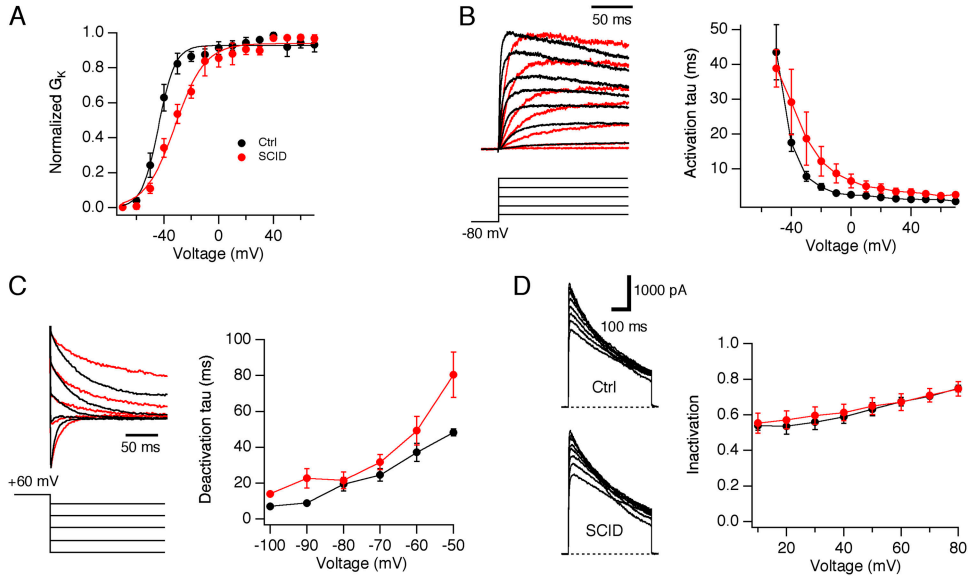

Figure 7. Voltage dependence and kinetics of Kv1.3 activation and deactivation are altered in SCID T cells. (A) The voltage sensitivity of Kv1.3 conductance in SCID cells is reduced. Kv1.3 conductance was measured from tail currents as described (see Materials and methods). Boltzmann curves were fitted and normalized to maximal conductance using the parameter values G_{max} = 8.85 nS, $V_{1/2}$ = −43.9 mV, and k = 6 mV (control) or G_{max} = 8.67 nS, $V_{1/2}$ = −31.6 mV, and k = 11 mV (SCID). (B) Activation kinetics of Kv1.3 current are slowed in SCID T cells. Currents evoked by pulses from −50 to +30 mV in control (black) and SCID T cells (red) are normalized to peak current at each voltage and superimposed (left). Activation kinetics were quantified by fitting single exponential functions to the final part of the rising phase of each current (right). (C) Deactivation kinetics are slowed in SCID cells. Normalized tail currents from a control (black) and a SCID T cell (red) upon repolarization to voltages of −100 to −50 mV (excluding −90 mV) after a 200-ms step to +60 mV are shown (left). Deactivation kinetics were measured from single exponential fits to each tail current (right). (D) Slow C-type inactivation of Kv1.3 current is not altered in SCID T cells. Currents from control (top) and SCID T cells (bottom) in response to 500-ms steps from +10 mV to +80 mV are shown (left). The extent of inactivation at the end of each pulse (right) is similar for control (black; *n* = 4 cells) and SCID cells (red; *n* = 5 cells).

ciated genes (8, 19). However, the precise nature of the Ca^{2+} influx defect was unknown, and several explanations for the phenotype were possible. We have shown here that TCR engagement or TG causes a normal amount of store depletion in the SCID cells, and hence, the influx defect does not seem to result from aberrant Ca^{2+} store regulation. In addition, expression of voltage-gated and Ca^{2+}-activated K^+ channels is normal, so that membrane depolarization and a reduced driving force for Ca^{2+} entry also is not a likely mechanism. Using patch-clamp recording, we provide the first direct evidence that the CRAC channels in the SCID T cells are not functional. CRAC-mediated currents were undetectable, even under conditions that offer the greatest sensitivity for detection (i.e., TG to deplete stores fully; a highly hyperpolarized potential to maximize driving force; a low concentration of 2-APB to enhance activity; and divalent-free extracellular conditions to enable Na^+ to permeate, and thereby, boost channel conductance). These measurements show unequivocally that the Ca^{2+} signaling defect in the cells is due to a failure of CRAC channels to open.

Importantly, these results also confirm the essential role of the CRAC channel in mediating Ca^{2+} influx in response to TCR stimulation. A recent study proposed that Ca_V channels underlie TCR-mediated Ca^{2+} entry in murine T cells (13), based on the endogenous expression of α and β subunits of L-type Ca^{2+} channels and depolarization-activated L-type Ca^{2+} currents in normal T cells, as well as abnormally small Ca^{2+} signals in response to TCR stimulation in mutant mice lacking the β4 subunit of the Ca^{2+} channel. These results are surprising considering that voltage-gated Ca^{2+} currents in T cells have not been detectable in a large number of electrophysiological studies, and membrane depolarization has never been shown to elevate $[Ca^{2+}]_i$ in T cells. In addition, it is not clear whether TCR cross-linking activates Ca_V channels. In the study by Badou et al. (13), anti-TCR antibodies evoked current fluctuations after an artificially imposed membrane depolarization but not at the cell's natural membrane potential. Finally, although normal and SCID human T cells express several isoforms of the Ca_V α1 subunit, thorough tests failed to reveal any Ca^{2+} current in response to depolarization before or after TCR stimulation (unpublished data). Further work is needed to understand the role of Ca_V channel proteins in human T cells, and to explore additional functions of the β subunits. In contrast, the absence of I_{CRAC} in SCID T cells clearly supports the idea that voltage-independent CRAC channels are the major, if not the sole, pathway for Ca^{2+} entry in response to stimulation through the TCR (43). Such a role also is consistent with previous studies of human SCID T cells (6, 7) and CRAC-deficient mutant Jurkat T cells (27, 44), in which a lack of CRAC channel activity was associated with the absence of TCR-mediated Ca^{2+} influx and deficient ac-

tivation of transcriptional pathways, cytokine secretion, and T cell activation.

The molecular basis of store-operated Ca^{2+} entry is one of the enduring mysteries of cell biology. Despite more than a decade of work by many laboratories focused on this question, little is known about the nature of the CRAC channel or its activation mechanism at a molecular level. Many genes and mechanisms have been proposed, but supporting evidence for many of these has been inconsistent. Of the TRP channels that have been suggested as candidates for CRAC channel subunits (TRPC1, TRPC3, TRPV6), we found that all were expressed in the SCID cells and did not display mutations, and that overexpression of TRPV6 was unable to rescue store-operated Ca^{2+} entry. The possible role of TRPV6 in CRAC channel formation is controversial. Early work indicated that TRPV6 shares several characteristic properties with CRAC, such as divalent cation selectivity, inactivation, and sensitivity to La^{3+} (11). In addition, overexpression of a dominant negative TRPV6 pore mutant was able to suppress endogenous I_{CRAC} in Jurkat cells (12); together, these studies supported the view that TRPV6 may encode at least part of the CRAC channel pore. However, other studies have shown differences with CRAC in terms of ion selectivity and rectification, effects of intracellular Mg^{2+} and 2-APB (15), and unitary conductance (25); furthermore, knockdown of TRPV6 with antisense or RNAi methods fails to reduce I_{CRAC} in RBL cells (45). Given the evidence that the SCID cells may bear a defect in the CRAC channel activation mechanism, our experiments do not exclude a role for TRPV6 in CRAC-mediated Ca^{2+} influx in normal lymphocytes; however, we reasonably can exclude their causative involvement in the CRAC deficiency in the SCID patients.

Which aspect of the CRAC channel activation process is deficient in the SCID T cells? The cells display a small amount of CRAC channel activity, identified by its store dependence and sensitivity to block by 2-APB, Gd^{3+}, La^{3+}, and SKF 96365; the properties of this residual Ca^{2+} influx can offer clues about the underlying defect. One possibility is that the CRAC channel is not expressed at the cell surface, because of a mutation affecting ion conduction, a defective promoter, or mutations interfering with transport and trafficking to the plasma membrane. If this were the case, the residual influx would represent a small number of normal channels, or a normal number of channels with greatly reduced ion conduction activity. One would predict that the activity of these channels would be enhanced by a low concentration of 2-APB (Fig. 3, E and F). This was not observed, arguing against the presence of a small number of otherwise normal CRAC channels in the plasma membrane.

An alternative explanation for this result is that the SCID cells harbor a defect in the CRAC channel activation process which impairs channel activity as well as the ability of 2-APB to enhance it. Recent evidence suggests that 2-APB inhibits several members of the TRP channel family by interfering with channel activation rather than blocking channel conduction itself. For example, 2-APB inhibits currents through *Drosophila* TRP channels activated by light or through mammalian TRPC3 channels activated by PLC-coupled receptors, but does not affect the same channels after they are activated directly by metabolic stress or diacylglycerol, respectively (46, 47). A defect in the activation machinery also may explain why store-operated Ca^{2+} influx was not observed in SCID T cells transfected with TRPV6. A defect in CRAC channel activation could occur at many levels between store depletion and channel opening, including the ER Ca^{2+} sensor, the proteins that communicate store depletion to the channel, and the ability of the CRAC channel itself to respond to the activation signal. Therefore, successful complementation of the SCID cells may reveal crucial information about the nature of the link between store depletion and channel activation, as well as the molecular mechanism of CRAC channel potentiation by 2-APB.

The expression and gross properties of several other channels (TRPM7, Kv1.3, and IKCa1) were normal in the SCID cells, suggesting that the mutation in the SCID cells specifically targets CRAC channel activation rather than channel expression, in general. However, we were surprised to find that the activation kinetics and voltage sensitivity of Kv1.3 are altered; the voltage sensitivity is reduced from a normal value of 6 mV per *e*-fold change in conductance to 11 mV, with a slowing of channel activation and deactivation. There are several ways in which Kv1.3 channels are known to be modulated in vivo. Association with β subunits promotes cell surface expression of the Kv1.3 α subunit, and thereby, increases current amplitude without altering the channel's voltage dependence or activation kinetics (48). Given that Kv1.3 current amplitude, cell surface expression of Kv1.3 (Fig. S4 C), and Kvβ1 and Kvβ2 expression are normal in the SCID T cells, a β subunit defect seems unlikely. Phorbol ester shifts the voltage dependence of Kv1.3 in T cells toward positive voltages but without the large decrease in voltage sensitivity (as indicated by the slope of the conductance-voltage curve) we have observed in SCID cells (49). Likewise, expression of *v-src* is known to cause a similar shift in voltage dependence without reducing voltage sensitivity, and also greatly slows the rate of inactivation, which also differs from the behavior of Kv1.3 in SCID cells (50). Thus, it seems unlikely that the abnormal K^+ channel properties observed in SCID T cells are simply due to altered phosphorylation by protein kinase C or a tyrosine kinase.

The association of altered K^+ channel kinetics with the lack of CRAC channel activity in SCID T cells suggests a functional link between CRAC and Kv channels. Although further work is needed to establish the nature of this link, one intriguing possibility is that Kv1.3 and CRAC channels are regulated by a common protein which is targeted by the SCID mutation. This protein target could be involved in posttranslational modification of both channels or could be a common subunit, adaptor, or scaffolding protein, which could influence clustering or activation of CRAC and Kv1.3. The PMCA and Kv1.3 bind to the scaffold MAGUK

protein SAP97 (hDlg) present in T cells (51, 52), and the sensitivity of PMCA in T cells to local gradients of Ca^{2+} near CRAC channels suggests that CRAC and PMCA are in close proximity to each other (53). These results raise the possibility that SAP97 may bring CRAC, PMCA, and Kv1.3 together in a multiprotein complex. Preliminary results suggest that the expression and localization of SAP97 are normal in SCID T cells and fibroblasts (unpublished data); thus, the SCID phenotype does not seem to involve a loss or gross mistargeting of SAP97. Further studies to examine the physical association of Kv1.3 with CRAC channels and other proteins in T cells may offer a new strategy for understanding the regulation of store-operated Ca^{2+} entry.

MATERIALS AND METHODS

Cells. Continuously growing T cell lines were derived from the peripheral blood lymphocytes of two patients and four healthy donors (22). Foreskin fibroblasts from newborn SCID patient 2 and a healthy newborn (Hs27 cell line, American Type Culture Collection) were immortalized by retroviral transduction with a telomerase expression plasmid (hTERT, gift of S. Lessnick, Dana-Farber Cancer Institute, Boston, MA). Patients in this study were included in a human subjects protocol which was reviewed and approved by the CBR Institute's internal review board. The rhabdomyosarcoma cell line TE671 was obtained from American Type Culture Collection.

Solutions and chemicals. Standard extracellular Ringer's solution contained (in mM): 155 NaCl, 4.5 KCl, 2 $CaCl_2$, 1 $MgCl_2$, 10 D-glucose, and 5 Na-Hepes (pH 7.4). In Ca^{2+}-free Ringer's, 1 mM EGTA + 2 mM $MgCl_2$ was substituted for $CaCl_2$. For measurements of I_{CRAC}, 20 mM $CaCl_2$ was used. DVF Ringer's solution contained (in mM): 155 Na methanesulfonate, 10 HEDTA, 1 EDTA, and 10 Hepes (pH 7.4 with NaOH). For measurements of K_{Ca} currents, NaCl in Ringer's solution was replaced with KCl. Internal solutions for recordings of I_{CRAC} contained (in mM): 150 Cs methanesulfonate, 8 $MgCl_2$, 10 BAPTA, and 10 Cs Hepes (pH 7.2). For recordings of I_{MIC}, internal solution contained (in mM): 150 Cs methanesulfonate, 10 HEDTA, 0.5 $CaCl_2$ and 10 Cs-Hepes (pH 7.2). For recordings of K_{Ca} current, internal solution contained (in mM): 150 K aspartate, 2 $MgCl_2$, 10 K Hepes, 10 EGTA, and added $CaCl_2$ to yield a free [Ca^{2+}] of 2 μM. For recordings of Kv1.3 current, internal solution contained (in mM): 150 K aspartate 4 $MgCl_2$, 10 EGTA, and 10 K Hepes. pH of all internal solutions was 7.2. Solutions were applied to the cells with a rapid multi-barrel local perfusion pipette (25). 2-APB was purchased from Sigma-Aldrich and TG was purchased from LC Biochemicals.

Cell extracts, immunoblotting, and immunocytochemistry. Preparation of total cellular extracts, immunoblotting, and immunocytochemistry was done as described (19) (see supplemental Materials and methods, available at http://www.jem.org/cgi/content/full/jem.20050687/DC1). Antibodies against STIM1 were obtained from BD Biosciences and as a gift of G. Velicelebi (Torrey Pines Therapeutics, La Jolla, CA). Antibody against calreticulin was purchased from Abcam (Cambridge, MA). For overexpression of STIM1, full-length STIM1 (NM_003156) cDNA (Openbiosystems) was subcloned into pENTR11 (Gateway system, Invitrogen) and transferred into MSCV-containing retroviral destination vector GFP-KV-DV for stable transduction of fibroblasts essentially as described (54). Immunocytochemical analysis was performed on an Axiovert S200 epifluorescence microscope (Carl Zeiss Microimaging, Inc.) with Openlab digital imaging software (Improvision); deconvolution of z-sections was performed to subtract out-of-focus signals.

Single-cell Ca^{2+} imaging. T cells were loaded with 1 μM fura-2/AM (Molecular Probes) in RPMI 1640 + 10% FBS for 30 min at 22–25°C, and fibroblasts grown directly on UV-sterilized cover slips were loaded with 3 μM fura-2/AM for 45 min at 22–25°C. Ca^{2+} imaging was done with a Zeiss Axiovert S200 epifluorescence microscope and OpenLab imaging software (Improvision) as described (8). To actively deplete Ca^{2+} stores, T cells were incubated with 5 μg/ml biotinylated anti-CD3 antibody (UCHT1, BD Biosciences) for 10 min at 22–25°C followed by cross-linking with 5 μg/ml streptavidin (Pierce Chemical Co.).

Patch-clamp electrophysiology. Whole-cell recording was conducted at 22–25°C using standard methods (25). Currents were filtered at 1 or 2 kHz with a 4-pole Bessel filter and sampled at 5 kHz. For measurements of CRAC and MIC currents, a voltage protocol consisting of a 100-ms step to −110 mV followed by a ramp from −110 to +90 mV lasting 100 ms was applied. Voltage pulses were delivered at 1-s intervals from a holding potential of +20 mV. Unless noted otherwise, all data were corrected for liquid junction potential of the pipette solution and for leak currents collected in Ca^{2+}-free Ringer's solution; averaged results are presented as the mean value ± SEM.

IKCa1 currents were measured by stepping the voltage to −100 mV for 100 ms followed by a ramp from −100 to +100 mV for 100 ms. For measurements of Kv1.3 currents, voltage pulses were delivered every 15–20 s from a holding potential of −80 mV, and currents were leak subtracted using the P/8 method with an offset of −20 mV. For conductance-voltage curves, tail currents were measured 200 μs after membrane repolarization. Curves were fit with a Boltzmann function: $G(V) = G_{max}/\{1 + \exp[(V\text{-}V_{1/2}/k)]\}$, where G_{max} is the maximal conductance, $V_{1/2}$ is the voltage for half-maximal activation, and k is the voltage sensitivity in mV.

Online supplemental material. Fig. S1 shows evidence that expression levels of IP_3 receptors and PLCγ are similar in control and SCID T cells. Fig. S2 quantitates store-operated Ca^{2+} influx in individual SCID T cells and shows that it is inhibited by 2-APB. Fig. S3 shows that expression levels of mRNA for TRPC1-5, TRPC7, TRPV5, and TRPV6 in SCID T cells are all within normal range. Fig. S4 shows evidence that protein expression of Kv1.3 and it's β subunits are normal in SCID calls, as are mRNA levels for Kv1.3, IKCa1, Kv3.1, and Kvβ1, β2, and β3. Online supplemental material is available at http://www.jem.org/cgi/content/full/jem.20050687/DC1.

The authors are grateful to members of the Lewis laboratory for helpful discussion. We thank M. Ohora for his excellent technical help with the STIM1 biochemical studies.

S. Feske was supported by a Cancer Research Institute postdoctoral fellowship, and M. Prakriya was supported by a postdoctoral fellowship from the Irvington Foundation for Immunological Research. This work was funded by National Institutes of Health grants AI054933 to S. Feske, HD39685 and AI40127 to A. Rao, and GM45374 to R.S. Lewis.

The authors have no conflicting financial interests.

Submitted: 5 April 2005
Accepted: 20 July 2005

REFERENCES

1. Hoth, M., and R. Penner. 1992. Depletion of intracellular calcium stores activates a calcium current in mast cells. *Nature*. 355:353–356.
2. Zweifach, A., and R.S. Lewis. 1993. Mitogen-regulated Ca^{2+} current of T lymphocytes is activated by depletion of intracellular Ca^{2+} stores. *Proc. Natl. Acad. Sci. USA*. 90:6295–6299.
3. Lewis, R.S. 2001. Calcium signaling mechanisms in T lymphocytes. *Annu. Rev. Immunol.* 19:497–521.
4. Bhakta, N.R., D.Y. Oh, and R.S. Lewis. 2005. Calcium oscillations regulate thymocyte motility during positive selection in the three-dimensional thymic environment. *Nat. Immunol.* 6:143–151.
5. Neilson, J.R., M.M. Winslow, E.M. Hur, and G.R. Crabtree. 2004. Calcineurin B1 is essential for positive but not negative selection during thymocyte development. *Immunity*. 20:255–266.
6. Partiseti, M., F. Le Deist, C. Hivroz, A. Fischer, H. Korn, and D. Choquet. 1994. The calcium current activated by T cell receptor and store depletion in human lymphocytes is absent in a primary immuno-

deficiency. *J. Biol. Chem.* 269:32327–32335.
7. Le Deist, F., C. Hivroz, M. Partiseti, C. Thomas, H.A. Buc, M. Oleastro, B. Belohradsky, D. Choquet, and A. Fischer. 1995. A primary T-cell immunodeficiency associated with defective transmembrane calcium influx. *Blood.* 85:1053–1062.
8. Feske, S., J. Giltnane, R. Dolmetsch, L. Staudt, and A. Rao. 2001. Gene regulation by calcium influx in T lymphocytes. *Nat. Immunol.* 2:316–324.
9. Mori, Y., M. Wakamori, T. Miyakawa, M. Hermosura, Y. Hara, M. Nishida, K. Hirose, A. Mizushima, M. Kurosaki, E. Mori, et al. 2002. Transient receptor potential 1 regulates capacitative Ca^{2+} entry and Ca^{2+} release from endoplasmic reticulum in B lymphocytes. *J. Exp. Med.* 195:673–681.
10. Philipp, S., B. Strauss, D. Hirnet, U. Wissenbach, L. Mery, V. Flockerzi, and M. Hoth. 2003. TRPC3 mediates T-cell receptor–dependent calcium entry in human T-lymphocytes. *J. Biol. Chem.* 278:26629–26638.
11. Yue, L., J.B. Peng, M.A. Hediger, and D.E. Clapham. 2001. CaT1 manifests the pore properties of the calcium-release-activated calcium channel. *Nature.* 410:705–709.
12. Cui, J., J.S. Bian, A. Kagan, and T.V. McDonald. 2002. CaT1 contributes to the stores-operated calcium current in Jurkat T-lymphocytes. *J. Biol. Chem.* 277:47175–47183.
13. Badou, A., S. Basavappa, R. Desai, Y.Q. Peng, D. Matza, W.Z. Mehal, L.K. Kaczmarek, E.L. Boulpaep, and R.A. Flavell. 2005. Requirement of voltage-gated calcium channel β4 subunit for T lymphocyte functions. *Science.* 307:117–121.
14. Kotturi, M.F., D.A. Carlow, J.C. Lee, H.J. Ziltener, and W.A. Jefferies. 2003. Identification and functional characterization of voltage-dependent calcium channels in T lymphocytes. *J. Biol. Chem.* 278: 46949–46960.
15. Voets, T., J. Prenen, A. Fleig, R. Vennekens, H. Watanabe, J.G. Hoenderop, R.J. Bindels, G. Droogmans, R. Penner, and B. Nilius. 2001. CaT1 and the calcium release-activated calcium channel manifest distinct pore properties. *J. Biol. Chem.* 276:47767–47770.
16. Venkatachalam, K., D.B. Van Rossum, R.L. Patterson, H.T. Ma, and D.L. Gill. 2002. The cellular and molecular basis of store-operated calcium entry. *Nat. Cell Biol.* 4:E263–E272.
17. Parekh, A.B., and R. Penner. 1997. Store depletion and calcium influx. *Physiol. Rev.* 77:901–930.
18. Prakriya, M., and R.S. Lewis. 2003. CRAC channels: activation, permeation, and the search for a molecular identity. *Cell Calcium.* 33:311–321.
19. Feske, S., R. Draeger, H.H. Peter, K. Eichmann, and A. Rao. 2000. The duration of nuclear residence of NFAT determines the pattern of cytokine expression in human SCID T cells. *J. Immunol.* 165:297–305.
20. Chandy, K.G., T.E. DeCoursey, M.D. Cahalan, C. McLaughlin, and S. Gupta. 1984. Voltage-gated potassium channels are required for human T lymphocyte activation. *J. Exp. Med.* 160:369–385.
21. Chandy, G.K., H. Wulff, C. Beeton, M. Pennington, G.A. Gutman, and M.D. Cahalan. 2004. K^+ channels as targets for specific immunomodulation. *Trends Pharmacol. Sci.* 25:280–289.
22. Feske, S., J.M. Muller, D. Graf, R.A. Kroczek, R. Drager, C. Niemeyer, P.A. Baeuerle, H.H. Peter, and M. Schlesier. 1996. Severe combined immunodeficiency due to defective binding of the nuclear factor of activated T cells in T lymphocytes of two male siblings. *Eur. J. Immunol.* 26:2119–2126.
23. Prakriya, M., and R.S. Lewis. 2001. Potentiation and inhibition of Ca^{2+} release-activated Ca^{2+} channels by 2-aminoethyldiphenyl borate (2-APB) occurs independently of IP_3 receptors. *J. Physiol.* 536:3–19.
24. Lepple-Wienhues, A., and M.D. Cahalan. 1996. Conductance and permeation of monovalent cations through depletion-activated Ca^{2+} channels (I_{CRAC}) in Jurkat T cells. *Biophys. J.* 71:787–794.
25. Prakriya, M., and R.S. Lewis. 2002. Separation and characterization of currents through store-operated CRAC channels and Mg^{2+}-inhibited cation (MIC) channels. *J. Gen. Physiol.* 119:487–507.
26. Hermosura, M.C., M.K. Monteilh-Zoller, A.M. Scharenberg, R. Penner, and A. Fleig. 2002. Dissociation of the store-operated calcium current I_{CRAC} and the Mg-nucleotide-regulated metal ion current MagNuM. *J. Physiol.* 539:445–458.
27. Fanger, C.M., M. Hoth, G.R. Crabtree, and R.S. Lewis. 1995. Characterization of T cell mutants with defects in capacitative calcium entry: genetic evidence for the physiological roles of CRAC channels. *J. Cell Biol.* 131:655–667.
28. Bautista, D.M., M. Hoth, and R.S. Lewis. 2002. Enhancement of calcium signalling dynamics and stability by delayed modulation of the plasma-membrane calcium-ATPase in human T cells. *J. Physiol.* 541: 877–894.
29. Aussel, C., R. Marhaba, C. Pelassy, and J.P. Breittmayer. 1996. Submicromolar La^{3+} concentrations block the calcium release-activated channel, and impair CD69 and CD25 expression in CD3- or thapsigargin-activated Jurkat cells. *Biochem. J.* 313(Pt 3):909–913.
30. Ross, P.E., and M.D. Cahalan. 1995. Ca^{2+} influx pathways mediated by swelling or stores depletion in mouse thymocytes. *J. Gen. Physiol.* 106:415–444.
31. Chung, S.C., T.V. McDonald, and P. Gardner. 1994. Inhibition by SK&F 96365 of Ca^{2+} current, IL-2 production and activation in T lymphocytes. *Brit. J. Pharm.* 113:861–868.
32. Ma, H.T., K. Venkatachalam, J.B. Parys, and D.L. Gill. 2002. Modification of store-operated channel coupling and inositol trisphosphate receptor function by 2-aminoethoxydiphenyl borate in DT40 lymphocytes. *J. Biol. Chem.* 277:6915–6922.
33. Freichel, M., S.H. Suh, A. Pfeifer, U. Schweig, C. Trost, P. Weissgerber, M. Biel, S. Philipp, D. Freise, G. Droogmans, et al. 2001. Lack of an endothelial store-operated Ca^{2+} current impairs agonist-dependent vasorelaxation in $TRP4^{-/-}$ mice. *Nat. Cell Biol.* 3:121–127.
34. Roos, J., P.J. Digregorio, A.V. Yeromin, K. Ohlsen, M. Lioudyno, S. Zhang, O. Safrina, J.A. Kozak, S.L. Wagner, M.D. Cahalan, et al. 2005. STIM1, an essential and conserved component of store-operated Ca^{2+} channel function. *J. Cell Biol.* 169:435–445.
35. Nadler, M.J., M.C. Hermosura, K. Inabe, A.L. Perraud, Q. Zhu, A.J. Stokes, T. Kurosaki, J.P. Kinet, R. Penner, A.M. Scharenberg, and A. Fleig. 2001. LTRPC7 is a Mg.ATP-regulated divalent cation channel required for cell viability. *Nature.* 411:590–595.
36. Runnels, L.W., L. Yue, and D.E. Clapham. 2001. TRP-PLIK, a bifunctional protein with kinase and ion channel activities. *Science.* 291: 1043–1047.
37. Kozak, J.A., H.H. Kerschbaum, and M.D. Cahalan. 2002. Distinct properties of CRAC and MIC channels in RBL cells. *J. Gen. Physiol.* 120:221–235.
38. Grissmer, S., B. Dethlefs, J.J. Wasmuth, A.L. Goldin, G.A. Gutman, M.D. Cahalan, and K.G. Chandy. 1990. Expression and chromosomal localization of a lymphocyte K^+ channel gene. *Proc. Natl. Acad. Sci. USA.* 87:9411–9415.
39. Grissmer, S., A.N. Nguyen, and M.D. Cahalan. 1993. Calcium-activated potassium channels in resting and activated human T lymphocytes. Expression levels, calcium dependence, ion selectivity, and pharmacology. *J. Gen. Physiol.* 102:601–630.
40. Leonard, R.J., M.L. Garcia, R.S. Slaughter, and J.P. Reuben. 1992. Selective blockers of voltage-gated K^+ channels depolarize human T lymphocytes: mechanism of the antiproliferative effect of charybdotoxin. *Proc. Natl. Acad. Sci. USA.* 89:10094–10098.
41. Kalman, K., M.W. Pennington, M.D. Lanigan, A. Nguyen, H. Rauer, V. Mahnir, K. Paschetto, W.R. Kem, S. Grissmer, G.A. Gutman, et al. 1998. ShK-Dap^{22}, a potent Kv1.3-specific immunosuppressive polypeptide. *J. Biol. Chem.* 273:32697–32707.
42. Beeton, C., H. Wulff, S. Singh, S. Botsko, G. Crossley, G.A. Gutman, M.D. Cahalan, M. Pennington, and K.G. Chandy. 2003. A novel fluorescent toxin to detect and investigate Kv1.3 channel up-regulation in chronically activated T lymphocytes. *J. Biol. Chem.* 278:9928–9937.
43. Lewis, R.S., and M.D. Cahalan. 1995. Potassium and calcium channels in lymphocytes. *Annu. Rev. Immunol.* 13:623–653.
44. Serafini, A.T., R.S. Lewis, N.A. Clipstone, R.J. Bram, C. Fanger, S. Fiering, L.A. Herzenberg, and G.R. Crabtree. 1995. Isolation of mutant T lymphocytes with defects in capacitative calcium entry. *Immunity.* 3:239–250.
45. Kahr, H., R. Schindl, R. Fritsch, B. Heinze, M. Hofbauer, M.E. Hack, M.A. Mortelmaier, K. Groschner, J.B. Peng, H. Takanaga, et al. 2004.

CaT1 knock-down strategies fail to affect CRAC channels in mucosal-type mast cells. *J. Physiol.* 557:121–132.
46. Chorna-Ornan, I., T. Joel-Almagor, H.C. Ben-Ami, S. Frechter, B. Gillo, Z. Selinger, D.L. Gill, and B. Minke. 2001. A common mechanism underlies vertebrate calcium signaling and *Drosophila* phototransduction. *J. Neurosci.* 21:2622–2629.
47. Ma, H.T., R.L. Patterson, D.B. van Rossum, L. Birnbaumer, K. Mikoshiba, and D.L. Gill. 2000. Requirement of the inositol trisphosphate receptor for activation of store-operated Ca^{2+} channels. *Science.* 287:1647–1651.
48. McCormack, T., K. McCormack, M.S. Nadal, E. Vieira, A. Ozaita, and B. Rudy. 1999. The effects of Shaker beta-subunits on the human lymphocyte K^+ channel Kv1.3. *J. Biol. Chem.* 274:20123–20126.
49. Chung, I., and L.C. Schlichter. 1997. Native Kv1.3 channels are upregulated by protein kinase C. *J. Membr. Biol.* 156:73–85.
50. Cook, K.K., and D.A. Fadool. 2002. Two adaptor proteins differentially modulate the phosphorylation and biophysics of Kv1.3 ion channel by SRC kinase. *J. Biol. Chem.* 277:13268–13280.
51. Kim, E., S.J. DeMarco, S.M. Marfatia, A.H. Chishti, M. Sheng, and E.E. Strehler. 1998. Plasma membrane Ca^{2+} ATPase isoform 4b binds to membrane-associated guanylate kinase (MAGUK) proteins via their PDZ (PSD-95/Dlg/ZO-1) domains. *J. Biol. Chem.* 273:1591–1595.
52. Hanada, T., L. Lin, K.G. Chandy, S.S. Oh, and A.H. Chishti. 1997. Human homologue of the *Drosophila* discs large tumor suppressor binds to p56lck tyrosine kinase and Shaker type Kv1.3 potassium channel in T lymphocytes. *J. Biol. Chem.* 272:26899–26904.
53. Bautista, D.M., and R.S. Lewis. 2004. Modulation of plasma membrane calcium-ATPase activity by local calcium microdomains near CRAC channels in human T cells. *J. Physiol.* 556:805–817.
54. Macian, F., F. Garcia-Cozar, S.H. Im, H.F. Horton, M.C. Byrne, and A. Rao. 2002. Transcriptional mechanisms underlying lymphocyte tolerance. *Cell.* 109:719–731.

Feske et al. www.jem.org/cgi/doi/10.1084/jem.20050687

Case report. Detailed case reports of the two SCID patients investigated in this study have been described (Feske, S., R. Draeger, H.H. Peter, K. Eichmann, and A. Rao. 2000. *J. Immunol.* 165:297–305; Feske, S., J.M. Muller, D. Graf, R.A. Kroczek, R. Drager, C. Niemeyer, P.A. Baeuerle, H.H. Peter, and M. Schlesier. 1996. *Eur. J. Immunol.* 26:2119–2126).

Antibodies and reagents. Antibodies against the following proteins were purchased: Kv1.3 (BD Biosciences); IP3R1 (Abcam); IP3R3 (Transduction Laboratories); PLCγ1, Kvβ2 (Upstate Biotechnology); PLCγ2 (Santa Cruz Biotechnology); and SAP97 (Stressgen). The following antibodies were gifts: Kvβ1.2 and Kvβ1.3 (W. Cole, University of Calgary, Calgary, Canada) and FAM-labeled ShK-F6CA sea anemone toxin specific for Kv1.3, purchased from Bachem. Thapsigargin (LC Biochemicals) was diluted from a 1 mM stock in DMSO. Charybdotoxin (Sigma-Aldrich) and ShK-DAP were diluted 1:1,000 from 50 μM or 200 nM stock solutions in water, respectively.

Cell extracts, immunoblotting, and immunocytochemistry. For immunoblotting, T cells were extracted at a concentration of 10^6 cells/10 μl in RIPA buffer (20 mM Tris, pH 7.5, 250 mM NaCl, 1 mM DTT, 10 mM $MgCl_2$, 1% NP-40, 0.1% SDS, and 0.5% sodium deoxycholate) supplemented with protease and phosphatase inhibitors as follows: 1 mM phenylmethyl sulfonyl fluoride (PMSF), 10 μg/ml aprotinin, 25 μM leupeptin, 10 mM NaF, 10 mM β-glycerophosphate, and 1 μM sodium orthovanadate. 10–50 μl of RIPA extracts were separated by 8–10% SDS-PAGE, and proteins were electrotransferred onto nitrocellulose membranes. For immunoblots, antibodies were diluted in TBS (10 mM Tris-HCl, pH 8.0, 150 mM NaCl) plus 5% milk. Blots were washed with TBS containing 0.05% Tween 20. Immunocytochemistry was done as described previously (Feske, S., R. Draeger, H.H. Peter, K. Eichmann, and A. Rao. 2000. *J. Immunol.* 165:297–305). In brief, T cells were spun onto poly-L-lysine–coated coverslips and fibroblasts were grown on UV-sterilized glass coverslips overnight. Cells were fixed using 3% paraformaldehyde and washed several times with 1× PBS + 0.5% NP-40 + 0.01% NaN_3. Cells were incubated with unconjugated protein-specific antibodies according to manufacturer's recommendations, washed, and incubated with secondary Cy-3–conjugated antibodies (Jackson ImmunoResearch Laboratories). For nuclear counterstaining, DAPI (Molecular Probes) was used at 1 μg/ml. Fluorescence was analyzed on an Axiovert S200 epifluorescence microscope (Zeiss) with Openlab digital imaging software (Improvision); deconvolution of z-sections was performed to subtract out-of-focus signals.

PCR, DNA sequencing and real-time PCR. Total RNA was prepared from T cells using Ultraspec reagent (Biotecx). cDNA was synthesized from total RNA using Superscript II reagent kit (Invitrogen). cDNA from two SCID patients, their parents, and at least two healthy controls was amplified by RT-PCR and sequenced for mutations in TRPC1, C3, TRPM2, TRPV5, and V6. Exon sequencing from genomic DNA of the above individuals was done for TRPC5, C6, TRPM5, TRPV5, and V6. All primer sequences are available upon request. Quantitative real-time PCR was performed using the iCycler system (BioRad Laboratories) with SYBR green PCR kit (Applied Biosystems). PCR efficiency was tested by serial dilutions and specificity of amplification was verified by melt curve analysis, restriction digests, and agarose gel electrophoresis of PCR products. SYBR green signals were captured at the end of each polymerization step (72°C). A threshold was set in the linear part of the amplification curve. Threshold cycles (C_T) for genes of interest were normalized to C_T for GAPDH house keeping gene control obtaining ΔC_T. Expression data were plotted as $0.5^{\Delta Ct} \times 10^6$, where 10^6 equals GAPDH cDNA expression levels. All primer sequences are available upon request.